Claudia Glasman
Universidad Autónoma de Madrid (Spain)

XXXIVth Rencontres de Moriond
QCD and High Energy Hadronic Interactions
Les Arcs, Savoie, France
March $20^{th} - 27^{th}$, 1999

Jet Production at HERA

from

H1 Collab.

ZEUS Collab.

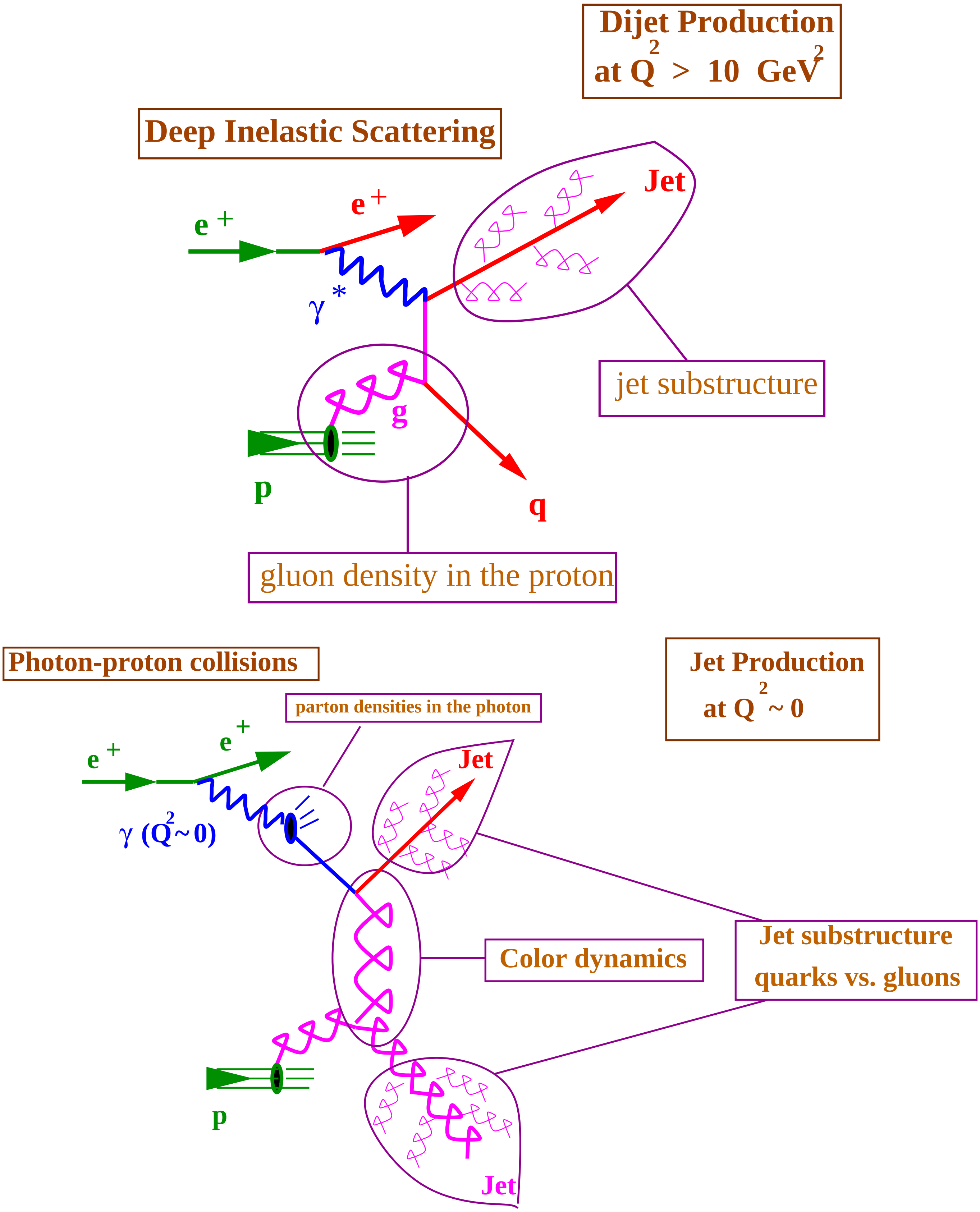
Dijet Production
at Q 2 > 10 GeV 2
Deep Inelastic Scattering
e +
e +
Jet
γ *
g
p
q
jet substructure
gluon density in the proton
Photon-proton collisions
parton densities in the photon
Jet Production
at Q 2 ~ 0
e +
e +
γ (Q 2 ~ 0)
Jet
Color dynamics
Jet substructure
quarks vs. gluons
p
Jet

Jet production in pQCD at LO α_s in photoproduction

- The **jet cross section in QCD** for the process $ep \to e + \text{jet}\ (+\text{jet}) + X$ in γp is given by two contributions:

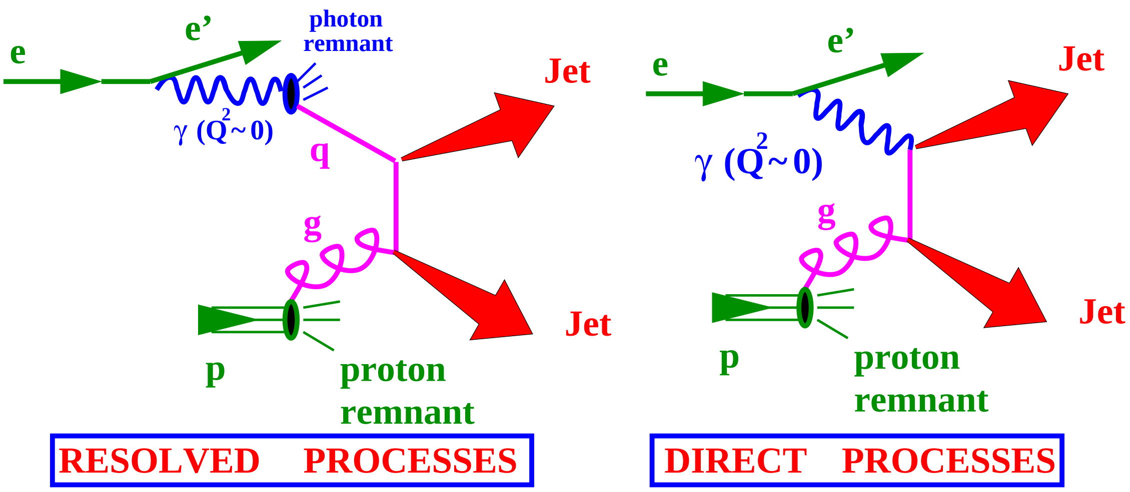

$$\sigma_{direct} = \int dPS\ f_{\gamma/e}(y)\ f_{j/p}(x_p, \mu^2) \times |M_{ij}(\cos\theta^*)|^2$$

$$\sigma_{resolved} = \int dPS\ f_{\gamma/e}(y)\ f_{j/p}(x_p, \mu^2) \times f_{i/\gamma}(x_\gamma, \mu^2)|M_{ij}(\cos\theta^*)|^2$$

$f_{\gamma/e}(y)$: flux of photons in e (Weizsaker-Williams approximation).

$f_{j/p}(x_p, \mu^2)$: parton densities in p (determined from other measurements (e.g., F_2^p)).

$f_{i/\gamma}(x_\gamma, \mu^2)$: parton densities in γ (partial information from other measurements (e.g., F_2^γ)).

$|M_{ij}(\cos\theta^*)|^2$: Matrix elements for the parton-parton scattering with scattering angle θ^* (pQCD).

Inclusive jet photoproduction

• Inclusive jet cross sections in γp are sensitive to the underlying parton dynamics and, therefore, provide a test of QCD and offer a potential means of studying the parton distributions in the photon.

• To test available parametrisations of the photon-parton densities we must reduce as much as possible the experimental and theoretical uncertainties.

• To reduce the uncertainty of the measurements due to a possible underlying event:
$\longrightarrow$ reduce cone radius ($R = 1.0 \rightarrow R = 0.7$, area of the cone is halved).
$\longrightarrow$ increase E_T^{jet} (as E_T^{jet} increases the jet pedestal stays approximately constant and becomes less relevant.)

Jet algorithm: k_T cluster algorithm
$\longrightarrow$ no merging
$\longrightarrow$ transparent translation of the theoretical jet algorithm to experimental setup
$\longrightarrow$ allows meaningful comparison with NNLO QCD calculations (when available)

Measurement of $\frac{d\sigma}{dE_T^{jet}}$ in photoproduction

- Jet search using the k_T cluster algorithm.
- Kinematic region: $0.2 < y < 0.85$

$$Q^2 \leq 4 \text{ GeV}^2$$

- $\frac{d\sigma}{dE_T^{jet}}$ for E_T^{jet} between 17 and 74 GeV, integrated over $-0.75 < \eta^{jet} < 2.5$.

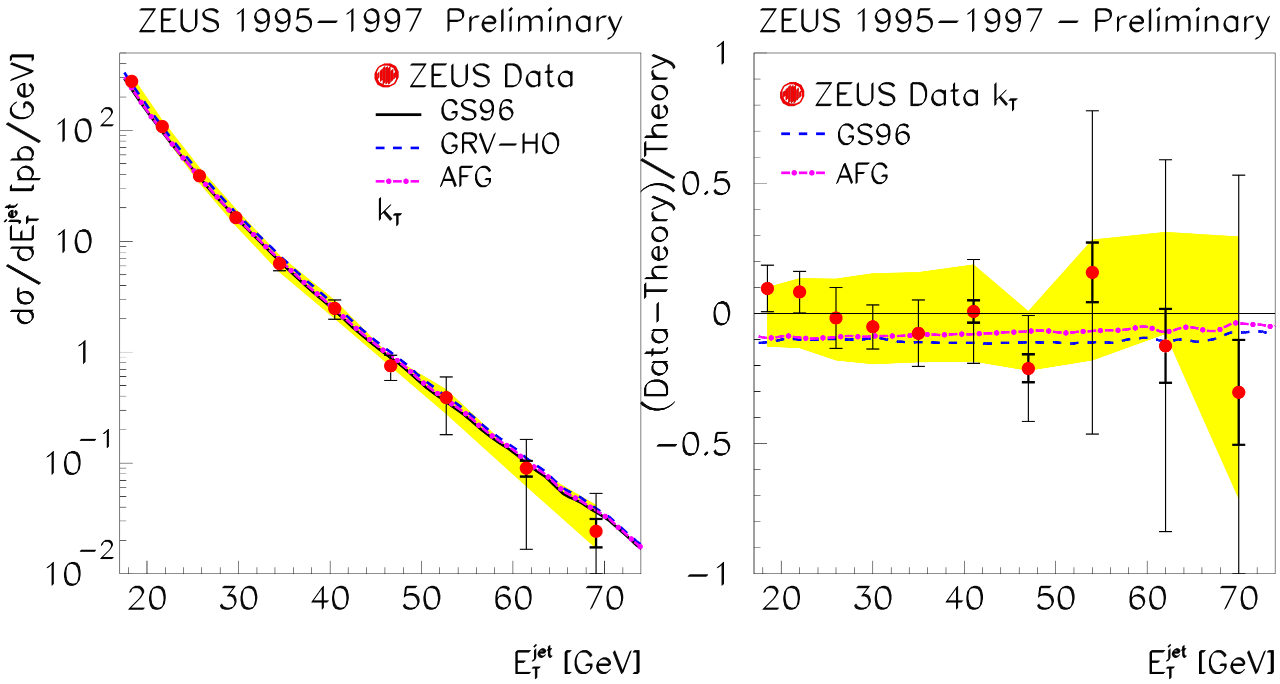

NLO QCD calculations by Harris & Owens and Klasen & Kramer

- The NLO calculations give a reasonable description of the measured differential cross section in magnitude and shape.

High-mass dijet cross sections in photoproduction

• The dijet mass (M^{JJ}) distribution provides a test of QCD and is sensitive to the presence of new particles or resonances that decay into two jets.

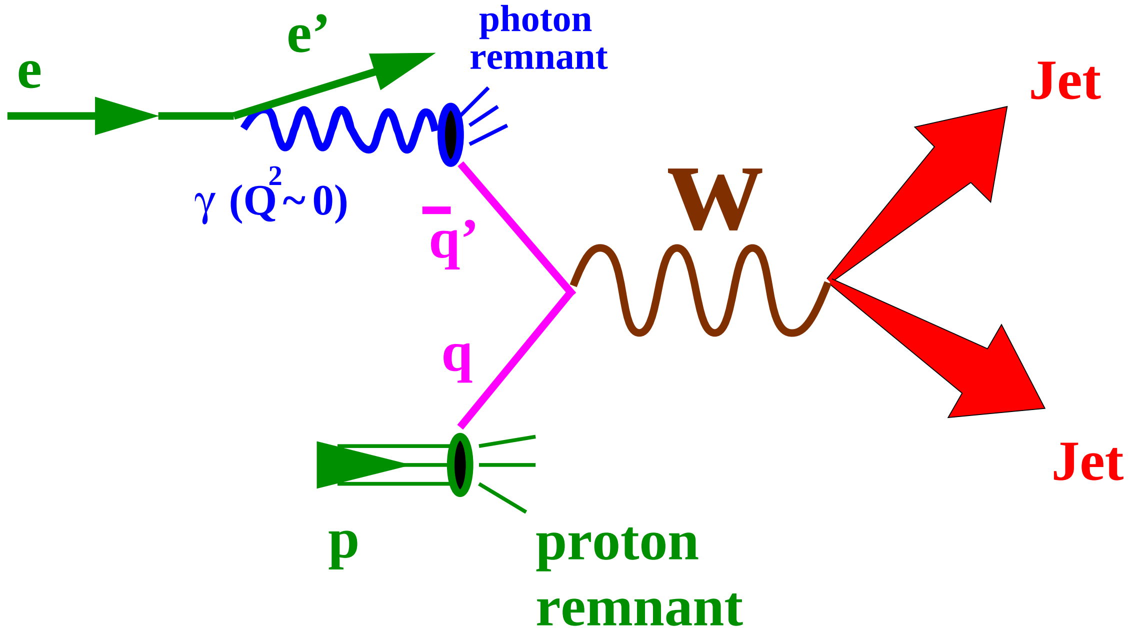

• The angular distribution in the dijet center-of-mass system ($\cos\theta^*$) reflects the underlying parton dynamics $\rightarrow$ sensitive to the spin of the exchanged particle.

• New particles or resonances decaying into two jets may also be identified by deviations in the measured $|\cos\theta^*|$ distribution w.r.t. QCD.

Measurement of high-mass dijet cross sections in γp

- 1995 to 1997 data (ZEUS) ($\mathcal{L} = 41$ pb^{-1})
- Jet search using the k_T cluster algorithm.
- Kinematic region: $0.2 < y < 0.85$

$$Q^2 \leq 4 \text{ GeV}^2$$

Dijet cross sections

- The two jets with highest E_T are selected and required to have: $E_T^{jet} > 14$ GeV

$$-1 < \eta^{jet} < 2.5$$

Measurements

- $\frac{d\sigma}{dM^{JJ}}$ for M^{JJ} between 47 GeV and 160 GeV, integrated over $|\cos\theta^*| < 0.8$.
- $\frac{d\sigma}{d|\cos\theta^*|}$ for $|\cos\theta^*|$ between 0 and 0.8, integrated over $M^{JJ} > 47$ GeV.

Measurement of $\frac{d\sigma}{dM^{JJ}}$ and $\frac{d\sigma}{d|\cos\theta^*|}$ in γp

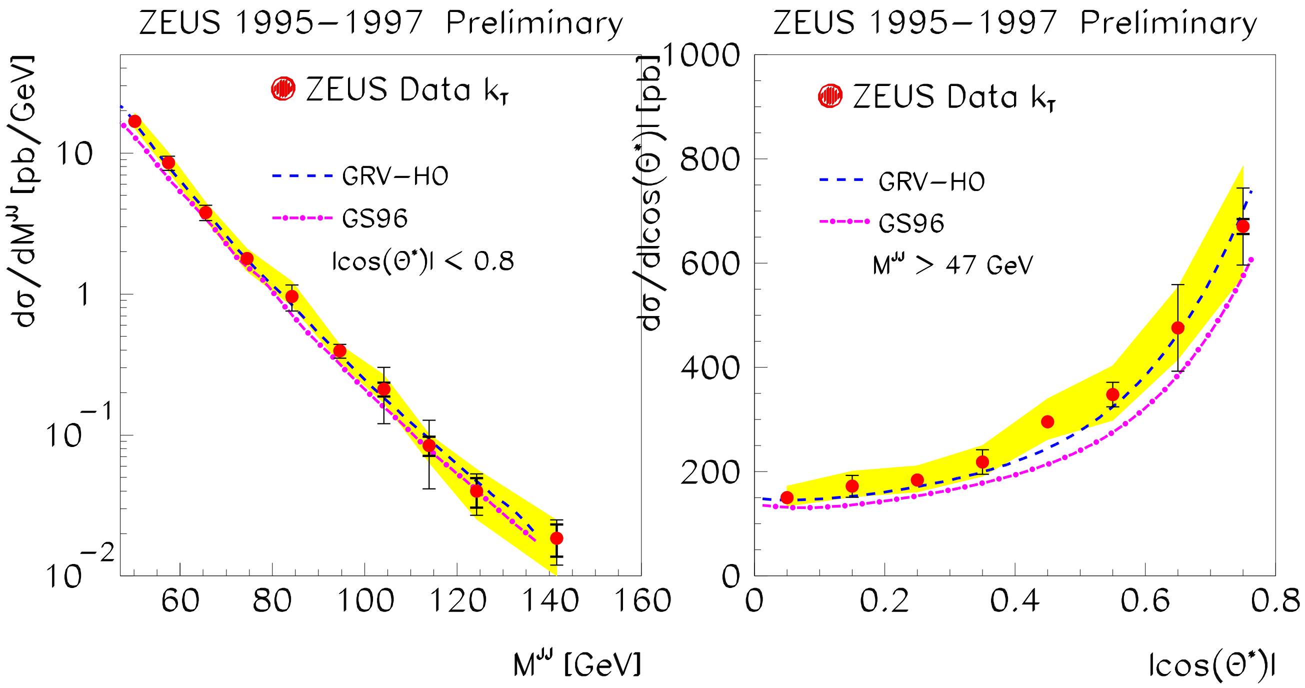

NLO QCD calculations vs. Data:

- The NLO calculations agree reasonably well in shape with the measured distributions $d\sigma/d|\cos\theta^*|$ and $d\sigma/dM^{JJ}$.
- The predictions based on GRV-HO are closer in magnitude to the measured cross sections.
- No significant deviation between data and NLO calculations is observed up to the highest M^{JJ} value studied and in the entire $|\cos\theta^*|$ range measured.

Jet shapes

- **Differential jet shape** ($\rho(r)$): average fraction of the jet transverse energy which lies in the annulus with inner (outer) radius $\mathrm{r}-\Delta\mathrm{r}/2$ $(\mathrm{r}+\Delta\mathrm{r}/2)$ concentric to the jet cone.

$$\boxed{\rho(r) = \frac{1}{N_{jets}\Delta r}\sum_{jets}\frac{E_T(r-\frac{\Delta r}{2}, r+\frac{\Delta r}{2})}{E_T(0,1)}}$$

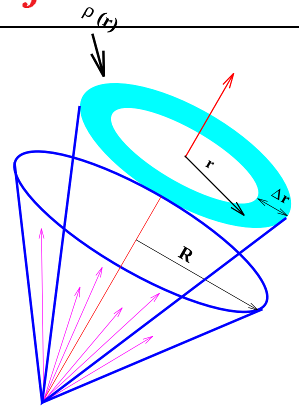

- **Integrated jet shape** ($\psi(r)$): average fraction of the jet's transverse energy inside an inner cone $r < R$, concentric with the jet defining cone.

$$\boxed{\psi(r) = \frac{1}{N_{jets}}\sum_{jets}\frac{E_T(0,r)}{E_T(0,1)}}$$

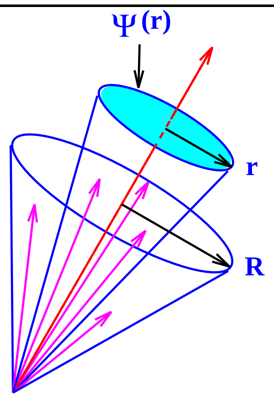

QCD predictions for the jet shape

• At sufficiently high E_T^{jet}, the jet shape is expected to be driven by gluon emission off the primary parton, and, therefore, calculable in perturbative QCD.

$\longrightarrow$ At LO QCD a jet consists of ONE parton and, thus, the jets have no structure.

$\longrightarrow$ NLO QCD calculations give the lowest non-trivial order contribution to the jet structure.

$\longrightarrow$ Calculations based on Monte Carlo Generators give an approximation to the jet structure by using parton showers.

• Gluon jets are predicted to be broader than quark jets due to the gluon-gluon coupling strength being larger than that of the quark-gluon.

Measurements of jet shapes in γp

- 1995 data (ZEUS) ($\mathcal{L} = 6$ pb^{-1})
- Jet search using the k_T cluster algorithm.
- Kinematic region: $0.2 < y < 0.85$
  $Q^2 \leq 4$ GeV^2

Differential and integrated jet shape

- Jets are required to have: $E_T^{jet} > 17$ GeV
  $-1 < \eta^{jet} < 2$

Measurements

- $\rho(r)$ in different η^{jet} regions.
- $\psi(r = 0.3)$ as a function of η^{jet}.

$\rightarrow$ Comparison with predictions from PYTHIA (QCD-based Monte Carlo which includes initial and final state radiation)

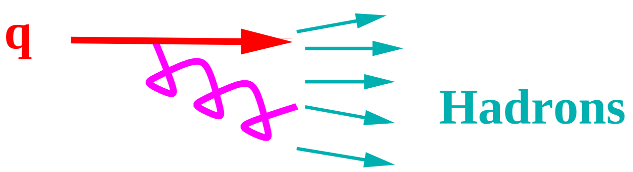

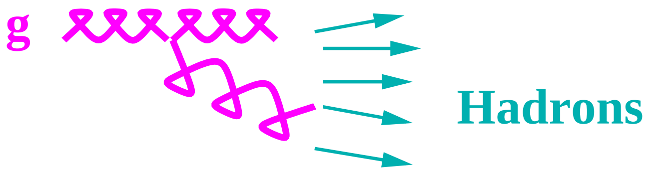

Jet shapes in γp: η^{jet} dependence

$(R = 1.0)$

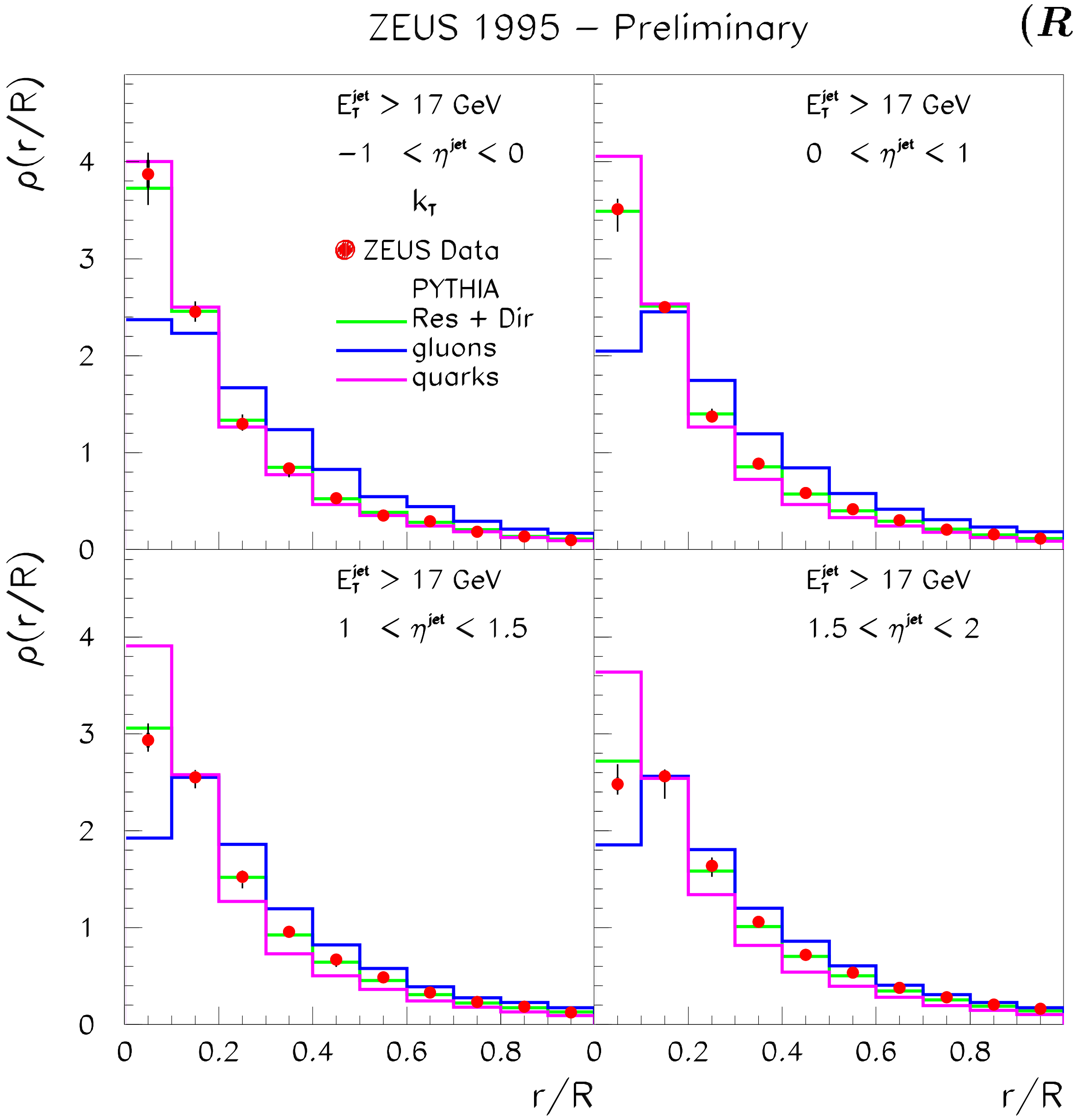

- Jets become broader as η^{jet} increases.
- Model including initial and final state QCD radiation give a good description of the data.
- The measured jets are

$\rightarrow$ quark-like for $-1 < \eta^{jet} < 0$

$\rightarrow$ more gluon-like for $1.5 < \eta^{jet} < 2$.

$\longrightarrow$ Challenge for NLO QCD calculations

Jet shapes in γp: η^{jet} dependence at fixed r

cone algorithm

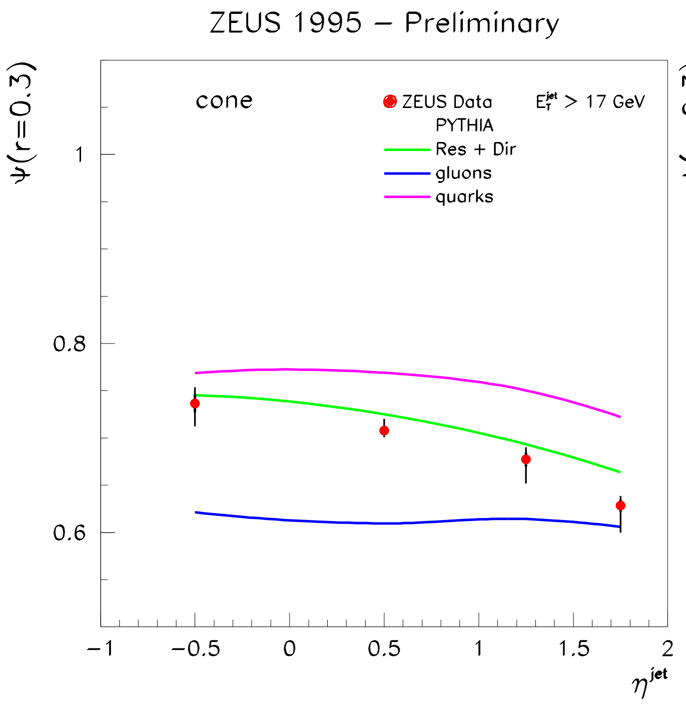

k_T algorithm

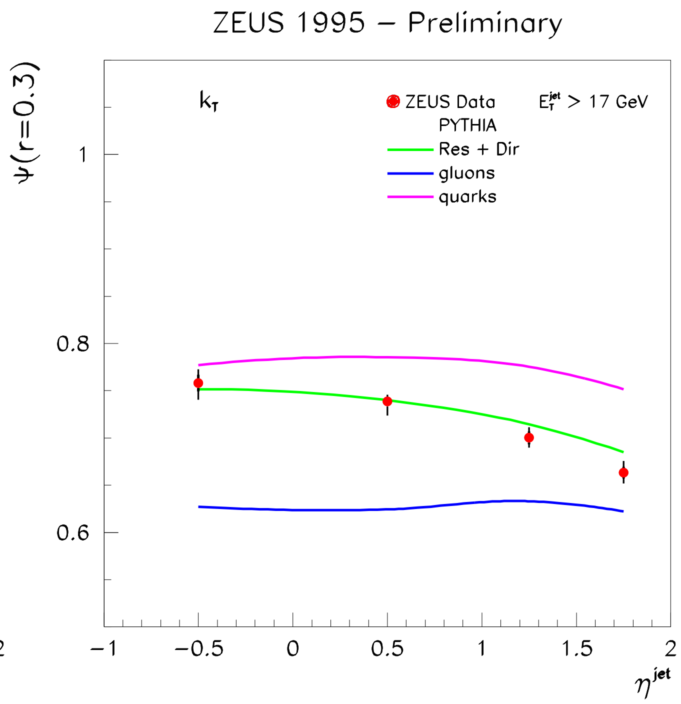

- The measured jet shape $\psi(r = 0.3)$ decreases with η^{jet}: the jets become broader as η^{jet} increases.
- The broadening of the jets (k_T and cone algorithms) is consistent with an increasing fraction of gluon-initiated jets as η^{jet} increases.
- The measured jet shapes with k_T and cone algorithms are similar for $r < 0.6$:
$\rho(k_T)/\rho(cone) \approx 1$ within $\pm 10\%$.

Dijet production in pQCD at LO α_s in DIS

- The jet cross section in QCD for the process $ep \to e + \text{jet} + \text{jet} + X$ in DIS is given by the contributions:

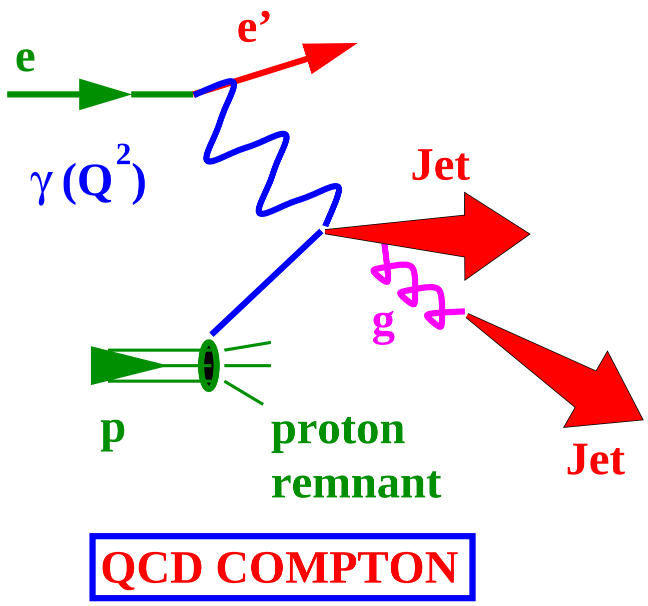

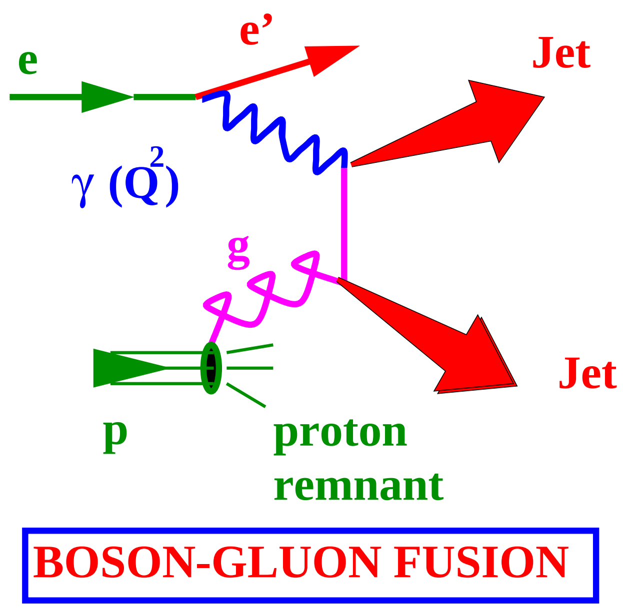

$$\sigma_{DIS} = \int dPS\, f_{i/p}(x_i, \mu_F^2) \times$$

$$d\hat{\sigma}^i(x_i \cdot P, \alpha_s(\mu_R^2), \mu_R^2, \mu_F^2)$$

$f_{i/p}$: parton densities in the proton.

$d\hat{\sigma}^i$: subprocess cross section.

Measurement of jet shapes in dijet production in DIS

- 1994 data (H1) ($\mathcal{L} = 2$ pb^{-1})

- Jet search using an iterative cone algorithm and the k_T cluster algorithm in the Breit frame.

- Kinematic region: $10 < Q^2 \lesssim 120$ GeV^2

$$2 \cdot 10^{-4} \lesssim x_{Bj} \lesssim 8 \cdot 10^{-3}$$

Integrated jet shape

- The two jets with highest E_T are selected and required to have: $E_{T,\mathrm{Breit}}^{jet} > 5$ GeV

$$-1 < \eta_{\mathrm{LAB}}^{jet} < 2$$

Measurements

- $\psi(r)$ as a function of $\eta_{\mathrm{Breit}}^{jet}$ and $E_{T,\mathrm{Breit}}^{jet}$.

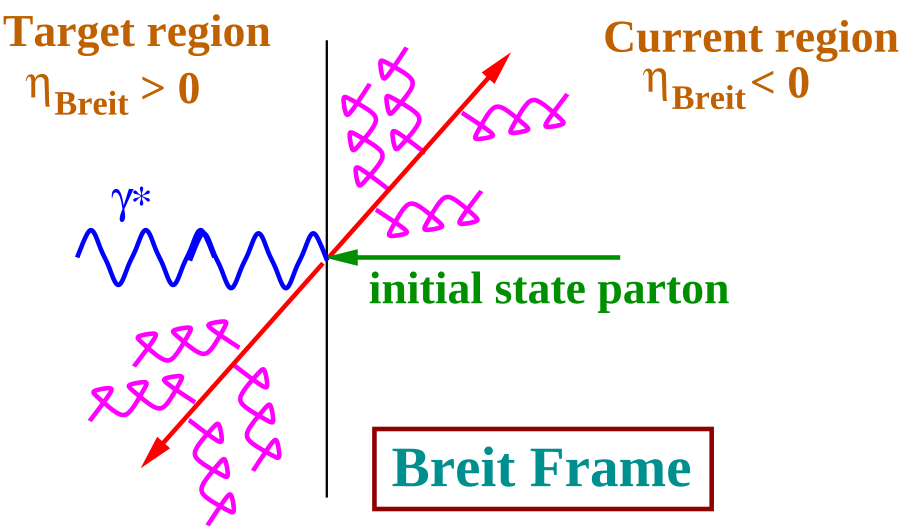

Jet shapes in NC DIS: $E_{T,\mathrm{Breit}}^{jet}$ and $\eta_{\mathrm{Breit}}^{jet}$ dependence

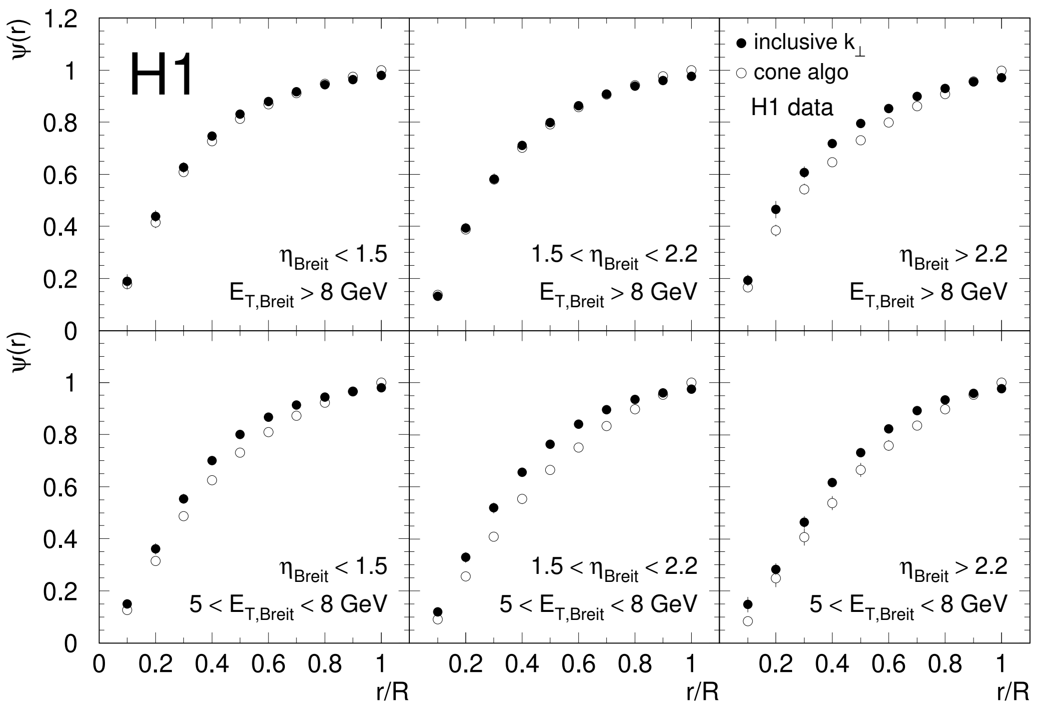

- Jets get narrower as $E_{T,\mathrm{Breit}}^{jet}$ increases.

- Jets get broader as $\eta_{\mathrm{Breit}}^{jet}$ increases (towards proton direction). The effect is more pronounced at low $E_{T,\mathrm{Breit}}^{jet}$.

- At low $E_{T,\mathrm{Breit}}^{jet}$ jets defined by the k_T cluster algorithm are narrower than jets defined by the cone algorithm.

- At high $E_{T,\mathrm{Breit}}^{jet}$ both jet algorithms produce very similar jets.

Jet Shapes in DIS

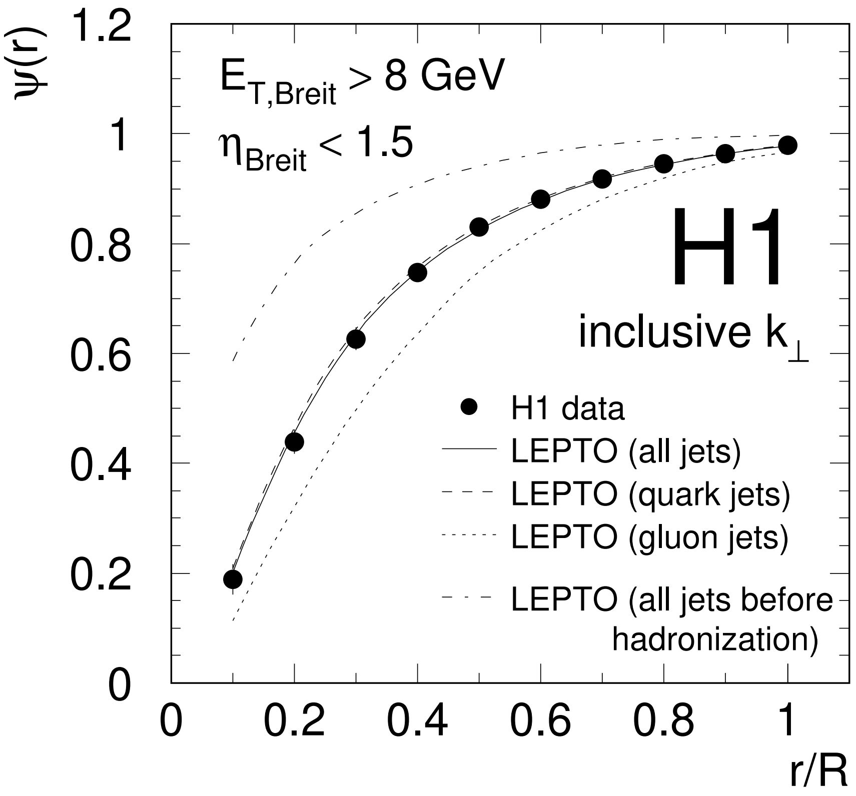

- **Model predictions:**

→ gluon jets are broader than quark jets.

→ in the kinematic region of the measurements, dijet sample is expected to be dominated by $q\bar{q}$ pairs.

- **The measured jet shape is compatible with that of quark initiated jets.**

Measurement of dijet cross sections in DIS

• 1994 to 1997 data (H1) ($\mathcal{L} = 36$ pb^{-1})

• Jet search using the k_T cluster algorithm in the Breit frame.

• Kinematic region: $0.2 < y < 0.6$

$$10 < Q^2 < 5000 \text{ GeV}^2$$

Dijet cross sections

• The two jets with highest E_T are selected and required to have: $E_{T,\mathrm{Breit}}^{jet} > 5$ GeV

$$E_{T,\mathrm{Breit}}^{jet1} + E_{T,\mathrm{Breit}}^{jet2} > 17 \text{ GeV}$$

$$-1 < \eta_{\mathrm{LAB}}^{jet} < 2.5$$

Measurements

• $\frac{d^2\sigma}{dQ^2 d\xi}$, where $\xi = x_{Bj}(1 + \frac{M_{JJ}^2}{Q^2})$.

• $\frac{d^2\sigma}{dQ^2 dx_{Bj}}$.

$\rightarrow$ Data corrected to hadron level.

$\rightarrow$ Data corrected for initial and final QED radiation.

Dijet Cross Sections in DIS

- **Hadronization effects small and independent of Q^2 $\longrightarrow$ compare data to DISENT** (NLO program from Catani & Seymour).

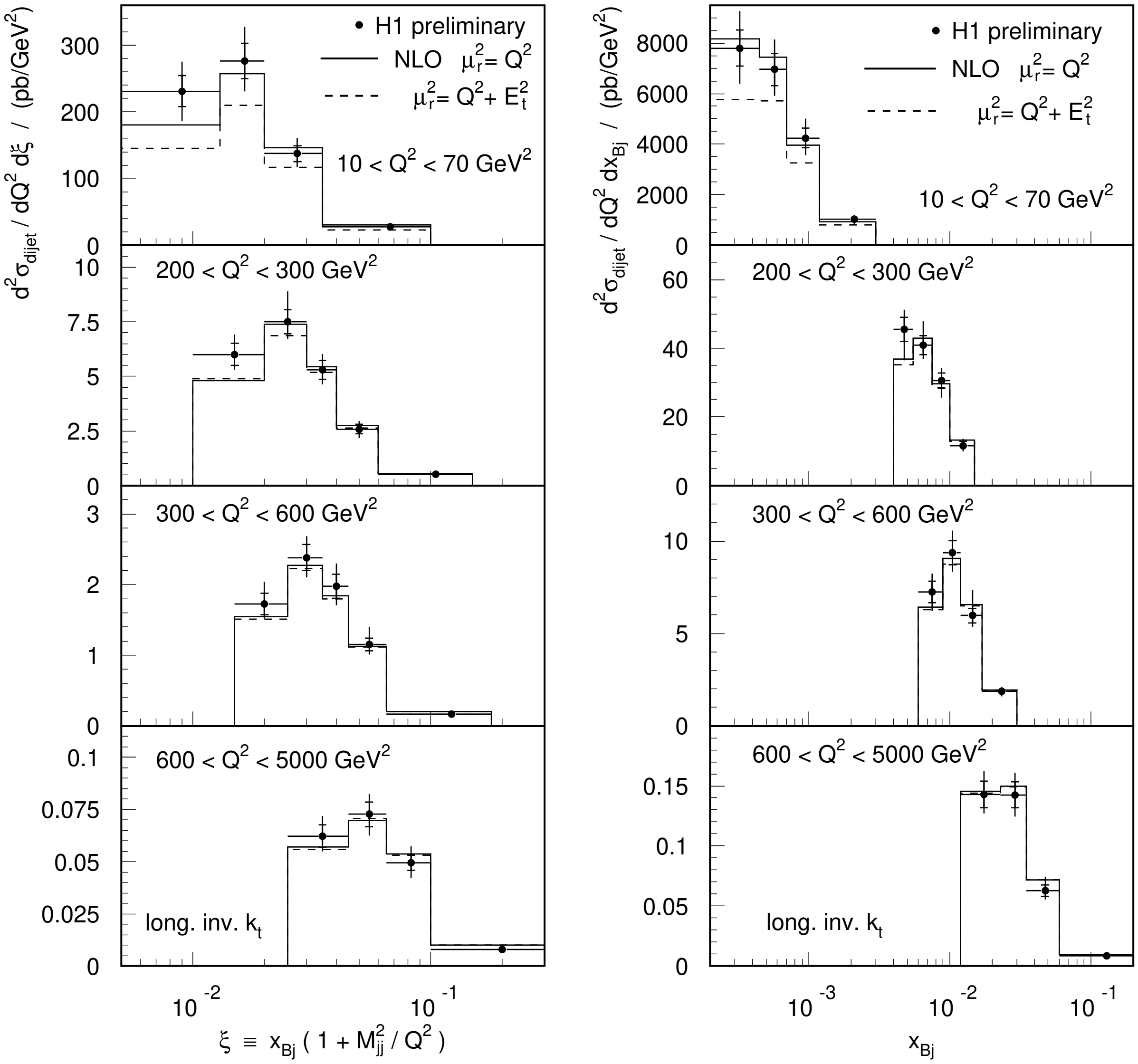

- **Small dependence of NLO calculations on μ_F (factorisation scale).**
- **Differences between different choices of μ_R (renormalisation scale) seen only at low Q^2.**
- **NLO predictions give a reasonable description of the data at all Q^2 for $\mu_R^2 = Q^2$.**

Gluon density in the proton

• Dijet cross sections sensitive to gluon and quark densities in the proton (the ξ and x_{Bj} distributions are most sensitive to the $x-$dependence of the parton densities in the region $0.01 \lesssim x \lesssim 0.2$).

$\rightarrow$ Direct determination of the gluon density in the proton from a QCD fit to the measured dijet cross sections.

• Inclusive NC DIS data sensitive to quark density. Include data at $200 \leq Q^2 \leq 650$ GeV^2 and $0.005 < x_{Bj} < 0.65$ to constrain quark density.

• Kinematic region of the measurement: $Q^2 > 200$ GeV^2.

$\rightarrow$ hadronization corrections are small ($\sim 7\%$) and flat in Q^2, ξ, x_{Bj}.

$\rightarrow$ theoretical scale uncertainties small.

Gluon density in the proton

- Use dijet cross sections and inclusive NC DIS data to perform a QCD fit and determine the gluon and quark densities in the proton at $\mu_F^2 = 200$ GeV^2 in the range $0.01 < x < 0.1$ for $\alpha_s(M_Z) = 0.119 \pm 0.005$.

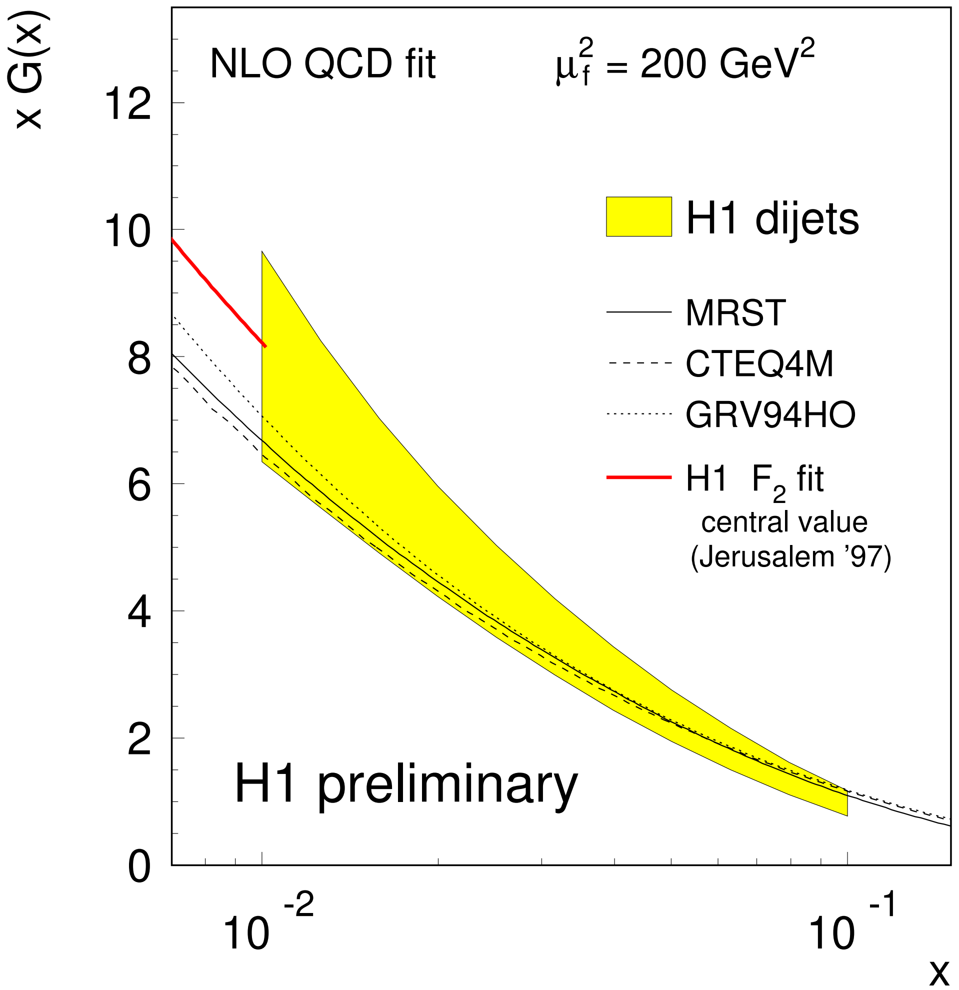

- Quark density 5% higher at $x = 0.01$ than results of global fits (CTEQ4M, MRST, GRV94HO) while in good agreement at $x = 0.1$.
- Gluon density slightly higher than results from global analyses (although compatible within the error) and in good agreement with determination from the QCD analysis of H1 F_2 at $x = 0.01$.

Conclusions

- Measurement of high-E_T jet cross sections in γp (ZEUS) using 1995 to 1997 data.
- Inclusive jet cross sections: reasonable description of the measured $d\sigma/dE_T^{jet}$ by NLO calculations up to 74 GeV.
- High-mass dijet cross sections: the NLO calculations describe reasonably well the shape and magnitude of the measured distributions $\rightarrow$ no significant deviation between data and calculations is observed up to $M^{JJ} \sim 140$ GeV.
- Measurement of jet shapes: consistent with an increasing fraction of gluon-jets as η^{jet} increases.

- Measurement of dijet cross sections in DIS (H1) using 1994 to 1997 data.
- Measurements of jet shapes in the Breit frame: consistent with those of quark initiated jets.
- Gluon density determined from a QCD fit to dijet and inclusive DIS data: compatible within errors with results from global analyses $\rightarrow$ universality of the gluon density.